ANALYSIS AND CALIBRATION OF DISCRETE ELEMENT PARAMETERS FOR *YANHUSUO* BASED ON STACKING TESTS

I

基于堆积试验的延胡索离散元参数分析与标定

Chun WANG[1,2], Xiangyang LIU[1], Yongchao SHAO[1], Weiguo ZHANG[*1]

[1]College of Mechanical and Electrical Engineering, Northwest Agriculture and Forestry University, Yangling 712100, China;
[2]College of Biological and Agricultural Engineering, Jilin University, Changchun 130000, China
Tel: +86-18291918130; E-mail: Wangchun11@nwafu.edu.cn
DOI: https://doi.org/10.35633/inmateh-76-28

Keywords: *Yanhusuo, discrete element, simulation parameter, calibration, stacking angle.*

ABSTRACT

To address the lack of contact parameters for yanhusuo during the mechanization process, its basic physical and contact parameters were derived through both theoretical calculations and practical measurements. Utilizing 3D scanning technology, a 3D model of yanhusuo was obtained. A discrete element model was then established using an automatic filling method. The key factors influencing the stacking angle of yanhusuo were identified using Plackett-Burman tests. The optimal ranges for these factors were determined through the steepest ascent experiment, and a quadratic regression model for the stacking angle was developed using response surface methodology (RSM) based on a rotational orthogonal experimental design. The optimized parameters - a restitution coefficient of 0.481, static friction coefficient of 0.508, and rolling friction coefficient of 0.029 - yielded a stacking angle of 21.23°. Experimental validation showed a relative error of just 0.86% between the simulation and physical tests. These results demonstrate that the discrete element model and calibrated parameters closely replicate real-world conditions, providing valuable insights for the mechanical design of yanhusuo planting and harvesting equipment.

摘要

针对延胡索机械化过程中延胡索接触参数缺乏的问题，通过理论计算和实际测量，推导了延胡索的基本物理参数和接触参数。利用 3D 扫描技术，获得延胡索的 3D 模型。采用自动填充法建立延胡索离散元模型。通过 Plackett-Burman 试验确定了影响延胡索堆积角的重要因素。通过最陡上升试验确定了这些重要因素的最佳范围，并通过旋转正交实验设计的响应面法（RSM）建立了与这些因素相关的堆积角的二次回归模型。优化后的参数—恢复系数为 0.481、静摩擦系数为 0.508、滚动摩擦系数为 0.029——产生的堆叠角为 21.23°。实验验证显示模拟与实际测试之间的相对误差为 0.86%。这些结果表明，离散元模型和校准参数密切复制了现实条件，为延胡索种植和收获的机械设计提供了宝贵的见解。

INTRODUCTION

Corydalis yanhusuo, a plant belonging to the Papaveraceae family and the Corydalis genus, is a traditional Chinese medicinal herb *(Chen et al., 2013; Ping et al., 2019*) that grows in loose, moist soils such as sandy or semi-sandy land. It typically has a flattened spherical shape, with a diameter ranging from 6 to 25 mm. *The yanhusuo* contains over 30 alkaloids, including tetrahydropalmatine and protopine, and exhibits significant pharmacological effects such as pain relief, sedation, and antiarrhythmic properties. As a result, *yanhusuo* hold considerable medicinal value *(Gu et al., 2020; Zhang et al., 2018*). In recent years, the increasing demand for *yanhusuo* due to its expanding applications in the pharmaceutical industry has led to a rise in its cultivation benefits. However, the seeding and harvesting of *yanhusuo* largely depend on manual labor, which presents challenges such as low efficiency and high costs. As an emerging economic crop, *yanhusuo* suffers from underdeveloped mechanization, and the lack of research in this field severely restricts the growth of the *yanhusuo* industry. Therefore, the mechanization of *yanhusuo* cultivation, from sowing to harvesting, is an urgent need. The accurate and objective collection of the mechanical parameters of *yanhusuo* is a prerequisite for developing specialized mechanized equipment.

Discrete Element Method (DEM) model and parameter calibration (*Ahmad et al., 2020; Horabik and Molenda, 2016; Mousaviraad and Tekeste, 2024; Ur Rehman et al., 2022*) are pivotal components in the simulation research of agricultural machinery. *Zhang et al., (2024),* developed a DEM model for red flowers, employing the Hertz-Mindlin (no slip) contact model to conduct packing angle tests and determine the optimal parameter set through orthogonal testing.

Chen et al., (2018), introduced a model approach for individual corn seeds and seed combinations, based on a classification of seed shapes, and validated their method through piling tests and "self-flow screening" tests. *Sun et al., (2022),* utilized the multi-sphere method to create wheat seed models consisting of 13, 17, 25, and 33 spheres. The accuracy and applicability of these models were verified through stacking angle simulations and physical tests. However, the *yanhusuo* exhibits a complex shape, and no DEM studies related to the *yanhusuo* have been reported, resulting in a lack of reference material. Therefore, the DEM model and parameters calibration for *yanhusuo* are critical for advancing simulation studies on this plant.

This study presents the determination of the fundamental physical and contact parameters for *yanhusuo* through theoretical analysis and empirical measurement tests. A multi-sphere bonded DEM model (*Guo et al., 2020; Ucgul et al., 2014, 2018; Wang et al., 2022; Xu B. et al., 2021; Xu T. et al., 2018*) for *yanhusuo* was established using the auto-filling method. The Plackett-Burman design and steepest ascent tests were employed to identify the significant factors affecting the packing angle of *yanhusuo* and their respective ranges. The optimal parameter combination was determined through an orthogonal rotation combination test. The reliability of the DEM model and contact parameters *(Katinas et al., 2019; Li et al., 2024; Poppa et al., 2024; Zhuang et al., 2023*) for the *yanhusuo* was further validated through test verification. The results provide fundamental parameters for simulating the mechanized seeding and harvesting of *yanhusuo*, offering a reference for the calibration of similar crops.

MATERIALS AND METHODS

Determination of basic physical parameters

The y*anhusuo* variety examined in this study is ZheHu No.1. The five-point sampling method was employed to collect a sample of *yanhusuo*, and its fundamental physical parameters were measured. A total of 50 *yanhusuo* were randomly selected and divided into five groups. Using an electronic balance with a precision of 0.01 g, the total mass of each group was measured and recorded. A graduated cylinder with a precision of 0.1 mL was filled with 98% ethanol to ensure complete submersion of the y*anhusuo* samples. The volume of each group was calculated by determining the difference between the initial and final readings of the graduated cylinder. Subsequently, the density of the *yanhusuo* was determined using the density formula, yielding a value of 1.085 g/cm³.

The moisture content of the *yanhusuo* is one of its fundamental parameters. In this study, an OHAUS MB23 rapid moisture analyzer was used to measure the moisture content of *yanhusuo*. The samples were divided into five groups for individual measurements, resulting in an average moisture content of 61.27%.

Poisson's ratio is the ratio of lateral strain to axial strain when a material is subjected to uniaxial compression (*Zhao et al., 2024*). It is a crucial mechanical characteristic parameter of *yanhusuo*. In this test, the compression deformation of *yanhusuo* was tested by Texture Analyzer. The Poisson's ratio of *yanhusuo* was calculated by measuring the deformation in the lateral (horizontal) and vertical (height) directions before and after loading, as shown in Figure 1.

Fig. 1- Compression test of *yanhusuo*

Before the test, the length and height of the *yanhusuo* were measured. At the start of tests, the *yanhusuo* was placed on the platform of Texture Analyzer. The compression head was manually adjusted to ensure its plane made contact with the upper surface of the *yanhusuo*. The experimental parameters were set with a loading rate of 0.5 mm/s and a loading duration of 3 seconds. After the test, the length and thickness of the

yanhusuo were measured again. The tests were repeated five times, and the average value was taken. The Poisson's ratio of the *yanhusuo* was calculated to be 0.49 using Eq.(1).

$$\lambda = \frac{\Delta L / L}{\Delta H / H} \quad (1)$$

where:

λ – Poisson's ratio;

ΔL – the absolute deformation in the direction of the length of the *yanhusuo*, mm;

L – the original length of the *yanhusuo*, mm;

ΔT – the absolute deformation in the direction of the height of the *yanhusuo*, mm;

T – the original length in the direction of the height of the *yanhusuo*, mm.

Young's modulus (*Khatchatourian et al., 2014; Shi et al., 2024*) is one of the mechanical characteristic parameters of the *yanhusuo*. In this study, Young's modulus of the *yanhusuo* was determined through compression testing by Texture Analyzer. The resulting compression force-displacement curve was obtained using the post-processing module of the computer software, as depicted in Figure 2.

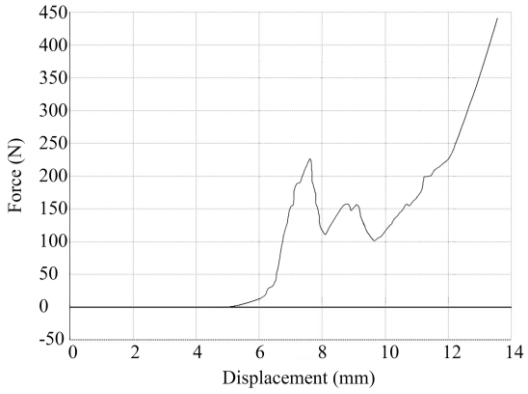

Fig. 2 - Load-displacement curve

The tests were repeated 5 times, the average value was calculated, and the Young's modulus of *yanhusuo* was calculated from Eq. (2) as *E* = 5.93 MPa

$$E = \left(\frac{\sigma}{A}\right) / v \quad (2)$$

where: E is the Young's modulus of the *yanhusuo*, [Pa]; σ is the maximum compressive stress, [kN]; A is the contact area of the compression head with the *yanhusuo* is 1.58 mm^2; v is the line strain.

Determination of contact parameters

Determination of the restitution coefficient

The restitution coefficient between the *yanhusuo* and steel plate was determined using a free-fall test (*Xu Bing et al., 2022)*. Before testing, the grid paper was positioned vertically on a horizontal surface, as illustrated in Figure 3. The *yanhusuo* sample was clamped at a height of H = 200 mm and released to fall freely. Upon impact with the steel plate, the rebound motion was captured using a high-speed camera system. The rebound height (h) was measured with the aid of graph paper and a ruler. This procedure was repeated ten times, and the average value was calculated.

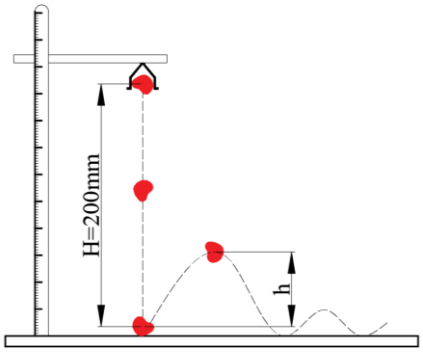

Fig. 3 - Schematic diagram of the test used to measure the restitution coefficient

The restitution coefficient can be calculated using the following formula:

$$e = \frac{v_4 - v_3}{v_2 - v_1} \quad (3)$$

$$v_4 = \sqrt{2gh} \quad (4)$$

$$v_2 = \sqrt{2gH} \quad (5)$$

where: e is the restitution coefficient between the *yanhusuo* and the colliding material; v_1 is the velocity of the colliding material before the collision, [mm·s^{-1}]; v_2 is the velocity of the y*anhusuo* before the collision, [mm·s^{-1}]; v_3 is the velocity of the colliding material after the collision, [mm·s^{-1}], v_4 is the velocity of the *yanhusuo* after the collision, [mm·s^{-1}]; H is the height from which the object is dropped before free fall, [mm]; h is the rebound height, [mm]; g is the gravity acceleration, [m·s^{-2}].

The measured restitution coefficient between *the yanhusuo* and the steel plate was 0.531.

Determination of the static friction coefficient

In this study, the inclined plane method was employed to measure the static friction coefficient between the *yanhusuo* and steel plate, as shown in Figure 4. By the hand-cranked mechanism, the angle of the inclined plane was gradually increased at a constant rate. The angle at which the tuber began to slide downward was recorded.

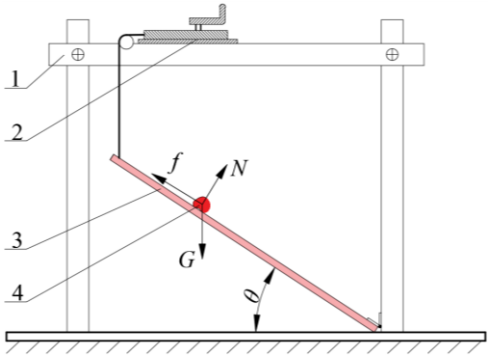

Fig. 4 - Static friction coefficient measurement test schematic

1. Rack; 2. Adjusting screws; 3. Inclined plane; 4. Yanhusuo.

Ten sets of tests were conducted for *yanhusuo* with steel plates, and the average values were calculated.

The formula for calculating the static friction coefficient is as follows:

$$f = G\sin\theta \quad (6)$$

$$F_N = G\cos\theta \quad (7)$$

$$\mu = \frac{F_N}{f} \quad (8)$$

where: f is the frictional force acting on *the yanhusuo*, [N]; G is the gravitational force on the *yanhusuo*, [N]; F_N is the support force acting on the *yanhusuo*, [N]; μ is the static friction coefficient; θ is the angle between the inclined plane and the horizontal surface, [°].

The average inclination angles for the *yanhusuo* tests with steel plate were substituted into Eq. (8) to calculate the static friction coefficients. The resulting static friction coefficient between *the yanhusuo* and the steel plate was 0.493.

Determination of rolling friction coefficient

The rolling friction refers to the resistance encountered when one object rolls on the surface of another without slipping, or when there is a tendency for rolling. It occurs as the contact surfaces of the two objects are compressed, resulting in deformation, which in turn generates a hindrance to the rolling motion. This study employs the bevel rolling method to measure the rolling friction coefficients between *the yanhusuo* and steel plate. As shown in Figure 5, where the angle between the inclined and horizontal planes is 30°. *The yanhusuo* was placed at a distance of L = 35 mm and allowed to roll freely with an initial velocity of 0 m/s until it came to a stop. The horizontal rolling distance(S) was subsequently measured. A total of 10 trials were conducted for each material.

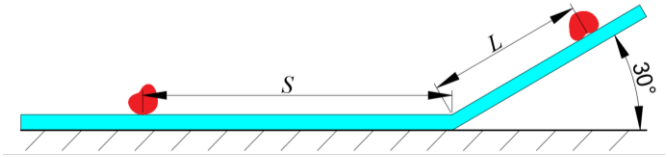

Fig. 5 - Schematic diagram of the method used to measure the rolling friction

The formula for calculating the rolling friction coefficient is as follows:

$$\mu' = \frac{GL\sin\beta}{G(L\cos\beta + S)} \tag{9}$$

where: G is the gravitational force on the *yanhusuo*, [N]; β is the angle of inclination of the inclined plane, [°]; S is the distance by the *yanhusuo* while rolling on a flat surface, [mm]; L is the distance by *the yanhusuo* while rolling on an inclined plane, [mm]; μ' is the rolling friction coefficient of *the yanhusuo* and the steel plate.

The rolling distance between *the yanhusuo* and the steel plate is 122.1 mm. Substituting these values into Eq. (9), the rolling friction coefficient between *the yanhusuo* and the steel plate is calculated to be 0.115.

The test for determining the stacking angle of *Yanhusuo*

In this study, data was initially obtained using the funnel method, followed by verification through the draw plate method. In the funnel method stacking test, the funnel, the base plate, and the baffle plate are all made of steel. The funnel has a height of 260 mm, a bottom diameter of 80 mm, and a top diameter of 240 mm. The funnel is positioned 150 mm above the base plate, with its discharge opening covered by the baffle plate. A total of 1000 *yanhusuo* are placed inside the funnel. The baffle plate is quickly removed, allowing *yanhusuo* to fall freely onto the base plate and accumulate. The test is shown in Figure 6.

Fig. 6 - Funnel method stacking test

1. Funnel; 2. Baffle plate; 3. Base plate; 4. Yanhusuo.

After photographing stacked *yanhusuo*, MATLAB image processing techniques are applied. Through binarization, edge detection is performed to extract the edge contour curve. A linear fit is then conducted to obtain the equation of the line, from which the stacking angle is calculated, as shown in Figure 7.

(a) Original image (b) Edge extraction and fitted image

Fig. 7 – *Yanhusuo* stacking angle

A total of 10 tests were conducted, with the slope values taken from both the left and right sides for each group. The final average value obtained was 21.05°.

Discrete element method modeling and simulation

The complex shape of *the yanhusuo* was addressed in this study by using 3D scanning imaging technology to capture their external contour models. The 3D contour models of *the yanhusuo* were exported in STL format. These files were imported into EDEM software, where a multi-sphere bonded particle model was applied, and the particle auto-fill method was used to construct the discrete element model of the *yanhusuo*, as illustrated in Figure 8.

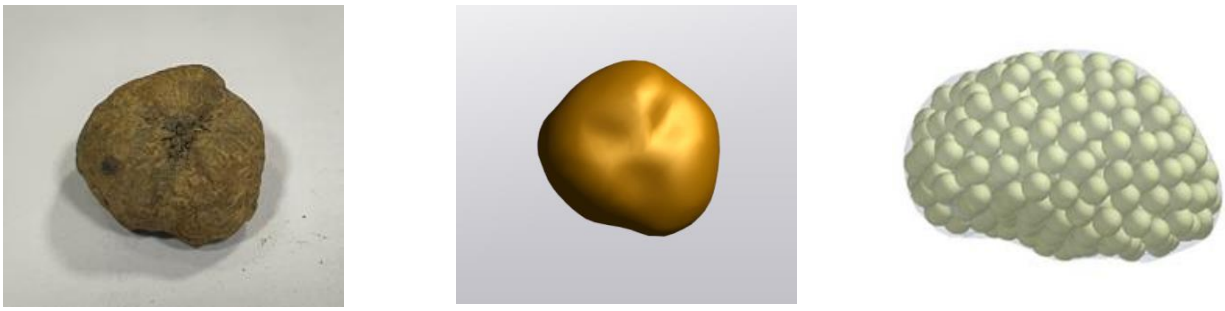

(a) *Yanhusuo* (b) Physical model © Discrete Element Model

Fig. 8 – *Yanhusuo* and discrete element model

The contact model between *the yanhusuo*, as well as between *the yanhusuo* and equipment components, was based on the Hertz-Mindlin contact theory. The material in contact with the *yanhusuo* is stainless steel, with the relevant parameters presented in Table 1.

Table 1

Simulation test parameters

Parameters	Numerical value
The Poisson's ratio of the y*anhusuo*	0.49
The density of the y*anhusuo,* [kg·m^{-3}]	1085
The Young's modulus of the *yanhusuo*, [Pa]	5.93×10^{6}
The Poisson's ratio of the steel	0.289
The density of the steel, [kg·m^{-3}]	7850
The Young's modulus of the steel, [Pa]	2.1×10^{11}

Parameter optimization for discrete element simulation

Plackett – Burman test

Plackett-Burman design was employed to screen for parameters that have a significant effect on the stacking angle. In the DEM simulation of y*anhusuo*, 8 parameters were selected as variable factors. The Plackett-Burman tested design was conducted using Design-Expert 13.0 software. A Plackett-Burman table with *N* = 12 was employed, with the stacking angle of *yanhusuo* as the response value. Each variable was set at two levels: high (+1) and low (-1). Table 2. provides an overview of the factors and levels used in the simulation.

Table 2

Plackett-Burman test measurement range table

Symbols	Test parameters	Low level (-1)	Hight level (+1)
A	Poisson's ratio of *the yanhusuo*	0.29	0.69
B	Young's modulus of the yanhusuo, [Mpa]	3.0×10^{6}	3.0×10^{7}
C	The collision recovery factor of *yanhusuo*	0.25	0.65
D	The coefficient of static friction of *yanhusuo*	0.35	0.75
E	The rolling friction coefficient of *yanhusuo*	0.005	0.045
F	*Yanhusuo*–steel plate collision recovery factor	0.3	0.8
G	*Yanhusuo*–steel plate coefficient of static friction	0.1	0.7
H	*Yanhusuo*–steel plate rolling friction coefficient	0.01	0.07

The steepest climb test

Based on the results of the Plackett-Burman test, significant factors were identified. Subsequently, the steepest ascent method was employed to quickly approach the optimal range of these significant factors.

Central composite design with quadratic orthogonal rotations

Based on the optimal factor level ranges identified through the steepest climb test, significant factors were selected for a central composite design with quadratic orthogonal rotations. Using the test results, a response surface model was fitted to derive the regression equation, which was then used to predict the optimal combination of simulation parameters for the *yanhusuo* that closely matches the actual stacking angle.

RESULTS AND DISCUSSION

Results of Plackett – Burman test

The results and analysis of variance for the Plackett-Burman test are presented in Tables 3 and 4. The results indicate that the restitution coefficient of *yanhusuo*, the static friction coefficient of *yanhusuo*, and the rolling friction coefficient of *yanhusuo* significantly influence the stacking angle, while other factors exhibit no significant effect. Therefore, the three significant factors identified above were selected for the steepest ascent tests.

Table 3

Design and results of the Plackett-Burman test

No.	*A*	*B*	*C*	*D*	*E*	*F*	*H*	*G*	Stacking angle
1	1	1	-1	1	1	1	-1	-1	22.72
2	-1	1	1	-1	1	1	1	-1	28.26
3	1	-1	1	1	-1	1	1	1	22.45
4	-1	1	-1	1	1	-1	1	1	20.35
5	-1	-1	1	-1	1	1	-1	1	27.14
6	-1	-1	-1	1	-1	1	1	-1	16.61
7	1	-1	-1	-1	1	-1	1	1	27.53
8	1	1	-1	-1	-1	1	-1	1	15.79
9	1	1	1	-1	-1	-1	1	-1	25.36
10	-1	1	1	1	-1	-1	-1	1	17.52
11	1	-1	1	1	1	-1	-1	-1	26.77
12	-1	-1	-1	-1	-1	-1	-1	-1	20.87

Table 4

Significance analysis of Plackett-Burman test parameters

Parameters	Degree of freedom	Sum of squares	F value	P value
A	1	8.12	2.91	0.1867
B	1	10.77	3.86	0.1443
C	1	46.53	16.66	0.0266*
D	1	28.61	10.25	0.0493*
E	1	97.30	34.84	0.0097**
F	1	2.46	0.8799	0.4174
G	1	7.92	2.84	0.1907
H	1	8.02	2.87	0.1887

*Note: *indicates that the impact was significant (P<0.05), and **indicates that the impact was extremely significant (P<0.01).*

Results of the steepest climb test

The design and results of the steepest climb test are shown in Table 5. The combination from group 3 yielded the smallest relative error in the stacking angle, with a value of only 1.08%. Therefore, Group 3 is selected as the zero level, and the optimal range of factor levels lies between group 2 and group 4.

Table 5

Scheme and results of the steepest climbing test

No.	Test factors			Result
	C	*D*	*E*	Relative Error (*Y*)
1	0.25	0.35	0.005	11.2206
2	0.35	0.45	0.015	6.8525
3	0.45	0.55	0.025	1.0847
4	0.55	0.65	0.035	4.1025
5	0.65	0.75	0.045	5.3476

The results of the second-order orthogonal rotating combination test

The results and analysis of variance for the three-factor, five-level orthogonal rotating combination test are presented in Tables 6 and 7.

Table 6

Test plan and results

No.	Test factors			Relative Error (Y)
	C	*D*	*E*	
1	-1	-1	-1	5.7982
2	1	-1	-1	8.6674
3	-1	1	-1	6.3763
4	1	1	-1	15.6287
5	-1	-1	1	8.4399
6	1	-1	1	1.5175
7	-1	1	1	4.5945
8	1	1	1	3.7030
9	-1.682	0	0	5.5840
10	1.682	0	0	7.9052
11	0	-1.682	0	2.7370
12	0	1.682	0	5.9228
13	0	0	-1.682	13.3637
14	0	0	1.682	6.2699
15	0	0	0	1.0018
16	0	0	0	2.1952
17	0	0	0	2.5026
18	0	0	0	1.3268
19	0	0	0	0.1075
20	0	0	0	0.9398

Using Design-Expert 13.0, the data in Table 6. was subjected to fitting analysis. The resulting regression equation for the relative error of the stacking angle, considering the collision restitution coefficient between *yanhusuo* (C), the static friction coefficient between *yanhusuo* (D), and the rolling friction coefficient between *yanhusuo* (E), is as follows:

$$Y = 1.36 + 0.6013C + 0.8228D - 3.31E + 1.55CD - 2.94CE - 1.15DE + 1.81C^2 + 0.9572D^2 + 2.90E^2 \quad (10)$$

The analysis of variance (ANOVA) for the regression equation is shown in Table 7. The coefficient of determination R^2 of the regression equation is 0.9713, indicating a high reliability of the model. The factors influencing the relative error of the stacking angle, in descending order of impact, are the rolling friction coefficient E, the static friction coefficient D, and the collision restitution coefficient C.

Table 7

ANOVA for quadratic equation models

Parameters	Sum of Squares	Degree of freedom	Mean square	F value	P value
Modal	319.13	9	35.46	72.39	<0.0001**
C	4.94	1	4.96	10.08	0.0099**
D	9.25	1	9.25	18.88	0.0015**
E	66.54	1	66.54	135.85	<0.0001**
CD	19.26	1	19.26	39.33	<0.0001**
CE	49.68	1	49.68	101.42	<0.0001**
DE	10.58	1	10.58	21.60	0.0009**
C^2	47.26	1	47.26	96.49	<0.0001**
D^2	13.20	1	13.20	26.96	0.0004**
E^2	120.96	1	120.96	246.95	<0.0001**
Residual	4.90	10	0.4898		
Lack of Fit	1.02	5	0.2043	0.2636	0.9152
Pure Error	3.88	5	0.7753		
Cor Total	324.03	19			

*Note: * indicates that the impact was significant (P<0.05), and **indicates that the impact was extremely significant (P<0.01).*

Parameter optimization

Based on the test results and the derived regression equation, the optimization function in Design-Expert 13.0 was used to minimize the relative error. The software was employed to search for the optimal combination of significant factors that yields the smallest relative error.

The objective function and constraints are as follows:

$$\begin{cases} \min Y(C,D,E) \\ \begin{cases} 0.282 \le C \le 0.618 \\ 0.382 \le D \le 0.718 \\ 0.008 \le E \le 0.042 \end{cases} \end{cases} \quad (11)$$

The optimized collision restitution coefficient between *yanhusuo* is 0.481, the static friction coefficient is 0.508, and the rolling friction coefficient is 0.029, with a relative error of the stacking angle of 0.804%. These parameters were input into the EDEM software, where 10 accumulation simulation trials were conducted. The average stacking angle obtained was 21.23°, with a relative error of only 0.86%. This indicates that the optimized parameter combination is highly reliable and can be used for subsequent DEM simulation tests.

Experimental validation

To further validate the authenticity of the *yanhusuo* discrete element simulation parameters, the board removal method was used for verification. A cuboid made of stainless steel was selected for the test. The dimensions of the cuboid are 150 mm in length, 150 mm in width, and 300 mm in height. A total of 1000 *yanhusuo* were placed inside. The baffle plate was quickly removed, allowing the *yanhusuo* to freely accumulate. The stacking angle was obtained using MATLAB image processing. Simultaneously, the corresponding DEM simulation was conducted. The test setup is shown in Figure 9.

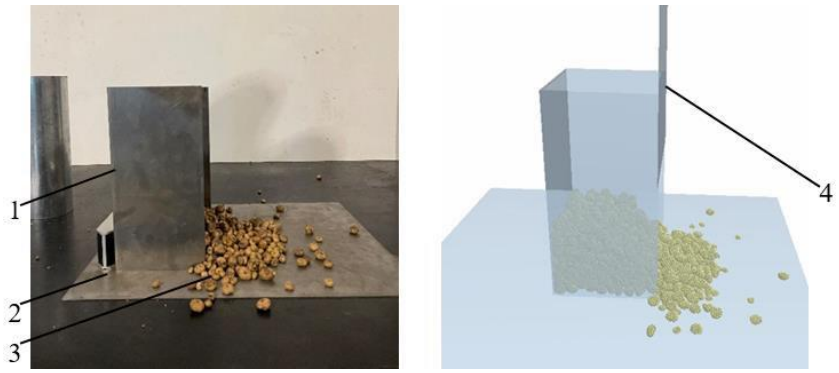

Fig. 9 - Measurement of *Yanhusuo* stacking angle by extraction plate method

1. Empty box of cuboids; 2. Base plate; 3. Yanhusuo; 4. Baffle plate.

Both types of tests were conducted for 10 trials each, and the average values were taken. The results are shown in Table 8.

Table 8

Actual and simulation test results of stacking angle by *Yanhusuo* draw plate method

No.	Actual test slope	Actual stacking angle / °	Simulation test slope	Simulation stacking angle / °
1	0.382	20.92	0.428	23.17
2	0.397	21.65	0.321	17.80
3	0.474	25.36	0.472	25.27
4	0.418	22.70	0.410	22.29
5	0.373	20.46	0.392	21.41
6	0.369	20.26	0.369	20.26
7	0.403	21.95	0.415	22.54
8	0.422	22.90	0.431	23.32
9	0.425	23.00	0.398	21.70
10	0.511	27.06	0.422	22.88
Average	**0.410**	**22.25**	**0.399**	**22.06**

The relative error between the actual measured stacking angle and the simulated value is 0.96%, indicating that the calibrated and optimized *yanhusuo* discrete element parameters can be reliably used for subsequent DEM simulations.

CONCLUSIONS

1. This study focuses on "Zhehu No. 1" as the research subject and conducts physical testing to determine the basic physical parameters of *yanhusuo*, including its density, moisture content, Young's modulus, and Poisson's ratio. Furthermore, the contact parameters between *yanhusuo* and steel plate were determined, including the restitution coefficient, static friction coefficient, and rolling friction coefficient.

2. The physical parameters of *yanhusuo* were selected as the simulation test parameters. Significant factors affecting the stacking angle were identified through the Plackett-Burman test, and the optimal range for these significant factors was further determined through the steepest ascent tests. Subsequently, a second-order orthogonal rotating combination test was conducted, with the minimization of the relative error in the stacking angle as the optimization objective, resulting in the optimal combination of simulation parameters.

3. The optimal parameter combination for *yanhusuo* was determined through calibration: a restitution coefficient of 0.481, a static friction coefficient of 0.508, and a rolling friction coefficient of 0.029. Verification tests showed that the relative error between the simulation and test tests was only 0.86%.

REFERENCES

[1] Ahmad, F., Qiu, B., Ding, Q., Ding, W., Khan, Z. M., Shoaib, M., Chandio, F.A., Rehim, A., Khaliq, A. (2020). Discrete element method simulation of disc type furrow openers in paddy soil. *International Journal of Agricultural and Biological Engineering*, *13*(4), 103–110.

[2] Chen, Y., Cao, Y., Xie, Y., Zhang, X., Yang, Q., Li, X., … Wang, S. (2013). Traditional Chinese medicine for the treatment of primary dysmenorrhea: how do *yuanhu* painkillers effectively treat dysmenorrhea? *Phytomedicine*, *20*(12), 1095–1104. https://doi.org/10.1016/j.phymed.2013.05.003

[3] Gu, Y., Huang, J., Guo, H., Song, X., Li, J., Shi, Y., Xie, X. (2020). A randomized controlled study for yuanhu zhitong dropping pills in the treatment of knee osteoarthritis. *Medicine*, *99*(24), e20666. https://doi.org/10.1097/MD.0000000000020666

[4] Guo, Y., Chen, Q., Xia, Y., Westover, T., Eksioglu, S., Roni, M. (2020). Discrete element modeling of switchgrass particles under compression and rotational shear. *Biomass and Bioenergy*, *141*, 105649. https://doi.org/10.1016/j.biombioe.2020.105649

[5] Horabik, J., Molenda, M. (2016). Parameters and contact models for DEM simulations of agricultural granular materials: a review. *Biosystems Engineering*, *147*, 206–225. https://doi.org/10.1016/j.biosystemseng.2016.02.017

[6] Katinas, E., Chotěborskỳ, R., Linda, M., Jankauskas, V. (2019). Wear modelling of soil ripper tine in sand and sandy clay by discrete element method. *Biosystems Engineering*, *188*, 305–319. https://doi.org/10.1016/j.biosystemseng.2019.10.022

[7] Khatchatourian, O. A., Binelo, M. O., de Lima, R. F. (2014). Simulation of soya bean flow in mixed-flow dryers using DEM. *Biosystems Engineering*, *123*, 68–76. https://doi.org/10.1016/j.biosystemseng.2014.05.003

[8] Li, Y., Zhou, W., Ma, C., Feng, Z., Wang, J., Yi, S., Wang, S. (2024). Design and optimization of the seed conveying system for belt-type high-speed corn seed guiding device. *International Journal of Agricultural and Biological Engineering*, *17*(2), 123–131. https://doi.org/10.25165/j.ijabe.20241702.8427

[9] Mousaviraad, M., Tekeste, M. Z. (2024). Systematic calibration and validation approach for discrete element method (DEM) modeling of corn under varying moisture contents (MC). https://doi.org/10.13031/ja.14763

[10] Ping, W., Tinglan, Z., Guohua, Y., Mengjie, L., Jin, S., Jiaqi, Z., … Hongjun, Y. (2019). Poly-pharmacokinetic strategy-delineated metabolic fate of bioactive compounds in a traditional Chinese medicine formula, yuanhu zhitong tablets, using parallel reaction monitoring mode. *Phytomedicine*, *53*, 53–61. https://doi.org/10.1016/j.phymed.2018.09.026

[11] Poppa, L., Frerichs, L., Liu, J., Böl, M. (2024). Development and implementation of a damage model for potato tuber blackspot in discrete element method to analyze harvesting and handling processes. *Journal of the ASABE*, 0. https://doi.org/10.13031/ja.15825

[12] Shi, Z., Wang, M., Zhang, X., Cheng, J., Lu, D. (2024). Calibration and optimization of discrete element parameters for coated cotton seeds. *Engenharia Agrícola*, *44*, e20230085. https://doi.org/10.1590/1809-4430-eng.agric.v44e20230085/2024

[13] Ucgul, M., Fielke, J. M., Saunders, C. (2014). Three-dimensional discrete element modelling of tillage: determination of a suitable contact model and parameters for a cohesionless soil. *Biosystems Engineering*, *121*, 105–117. https://doi.org/10.1016/j.biosystemseng.2014.02.005

[14] Ucgul, M., Saunders, C., Fielke, J. M. (2018). Comparison of the discrete element and finite element methods to model the interaction of soil and tool cutting edge. *Biosystems Engineering*, *169*, 199–208. https://doi.org/10.1016/j.biosystemseng.2018.03.003

[15] Ur Rehman, A., Awuah-Offei, K., Sherizadeh, T., Guner, D. (2022). Use of scaled discrete element model of rubber tire loader buckets for draft prediction. *Biosystems Engineering*, *214*, 1–10. https://doi.org/10.1016/j.biosystemseng.2021.12.003

[16] Wang, S., Yu, Z., Zhang, W. (2022). Study on the modeling method of sunflower seed particles based on the discrete element method. *Computers and Electronics in Agriculture*, *198*, 107012. https://doi.org/10.1016/j.compag.2022.107012

[17] Xu, B., Zhang, Y., Cui, Q., Ye, S., Zhao, F. (2021). Construction of a discrete element model of buckwheat seeds and calibration of parameters. *INMATEH-Agricultural Engineering*, *64*(2). https://doi.org/10.356.33/inmateh-64-17

[18] Xu, T., Yu, J., Yu, Y., Wang, Y. (2018). A modelling and verification approach for soybean seed particles using the discrete element method. *Advanced Powder Technology*, *29*(12), 3274–3290. https://doi.org/10.1016/j.apt.2018.09.006

[19] Xu, B., Zheng, D., Cui, Q. (2022). Experimental research on three-level vibrating screening of buckwheat based on discrete element method. *INMATEH-Agricultural Engineering*, *68*(3), pp.191-200. https://doi.org/10.35633/inmateh-68-19

[20] Zhang, H., Wu, X., Xu, J., Gong, S., Han, Y., Zhang, T., Liu, C. (2018). The comparative pharmacokinetic study of yuanhu zhitong prescription based on five quality-markers. *Phytomedicine*, *44*, 148–154. https://doi.org/10.1016/j.phymed.2018.02.005

[21] Zhao, J., Yu, J., Sun, K., Wang, Y., Liang, L., Sun, Y., … Yu, Y. (2024). A discrete element method model and experimental verification for wheat root systems. *Biosystems Engineering*, *244*, 146–165. https://doi.org/10.1016/j.biosystemseng.2024.06.004

[22] Zhuang, H., Wang, X., Zhang, X., Cheng, X., Wei, Z. (2023). Discrete element-based design of key parameters for wheel rut tillage devices. *Engenharia Agrícola*, *43*(3), e20230039. https://doi.org/10.1590/1809-4430-eng.agric.v43n3e20230039/2023